International Journal of Fluid Power 5 (2004) No. 3 pp. 39-48

DESIGN AND EXPERIMENTAL EVALUATION OF POSITION CONTROLLERS FOR HYDRAULIC ACTUATORS: BACKSTEPPING AND LQR-2DOF CONTROLLERS

Ana Lúcia Driemeyer Franco*, Edson Roberto De Pieri*, Eugênio Bona Castelan*, Raul Guenther and Antônio Carlos Valdiero****

** Federal University of Santa Catarina (UFSC), DAS/CTC, Florianópolis, 88040-900 SC, Brazil*
*** Federal University of Santa Catarina (UFSC), EMC/CTC, Florianópolis, 88040-900 SC, Brazil*
analucia@das.ufsc.br, edson@das.ufsc.br, eugenio@das.ufsc.br, guenther@emc.ufsc.br, valdiero@emc.ufsc.br

Abstract

In this paper the problem of experimental control of hydraulic actuators is considered. To deal with mechanical and hydraulic uncertainties two different controllers are synthesized: a backstepping controller and a LQR-2DOF controller. Experimental results of both implementations are analyzed in the context of practical difficulties, mainly the measurement of acceleration. These results illustrate the main features of these controllers when applied on a hydraulic actuator.

Keywords: hydraulic actuators, nonlinear control, Lyapunov based design, backstepping, linear control, 2DOF control design, robustness, disturbance rejection

1 Introduction

Hydraulic actuators are largely employed in industry. These actuators have high durability and high power density, providing large forces at high speeds with a relatively small size, which is an advantage when compared to electric and pneumatic actuators. For such reasons, hydraulic actuators (and hydraulic motors) are used in machine tools, in robot manipulators (Heintze, 1997) and in vehicle suspensions (Fialho and Balas, 1998; Wang and Wilson, 2001). However, hydraulic actuators present a highly nonlinear behaviour (due to the pressure-dependent compressibility of the fluid, to the nonlinear flow equations and to the friction forces acting on the cylinder), along with lightly damped dynamics and parameter variations. These characteristics are obstacles for the design of adequate controllers, especially in applications that require high performance such as, for example, robotic systems, since a hydraulic robot will have its behaviour dominated by the actuator dynamics.

In order to overcome these obstacles, many kinds of controllers for hydraulic actuators have been proposed in the literature. A review of the research on the control of fluid power systems was presented by Edge (1997). As stated by him, the linearised model has a single pole in the origin and two complex conjugate poles badly damped. In Guenther et al (2000), it is shown that the poles and zeros added in the closed-loop by classical controllers (like P, PD, PI and PID) do not change appropriately the location of the complex conjugate poles. Therefore, these controllers achieve only limited performance. Furthermore, the robustness requirements are hardly achieved. In order to improve the closed-loop performance, most controllers take into account the nonlinear nature of this actuator. In Guenther et al (1998), a cascade control was proposed, with the hydraulic subsystem being separated from the mechanical subsystem and controlled by a variable structure controller. Lyapunov based nonlinear controllers designed using the backstepping methodology were first studied by Yao et al (1998), who presented only simulation results. In Sirouspour and Salcudean (2000), experimental results for such controllers were presented. Even though the results were satisfactory, the large number of numerical differentiations required may pose a problem for practical implementation, because of the amplification of noises caused by such derivations. Another Lyapunov based nonlinear controller, which used a technique similar to backstepping for the design, was proposed by Sohl and Bobrow (1999). In order to cope with parameter variations, adaptive controllers that identify the parameter values on line were used in Bobrow and Lum (1995), Rudas et al (2003) and Yao et al (2000). All the controllers mentioned above control the actuator position.

This manuscript was received on 14 August 2004 and was accepted after revision for publication on 15 October 2004

In Jovanović (2002), the backstepping methodology was used to design a velocity controller for a hydraulic motor, which showed good results in simulations. Many other works deal with force control.

In this paper, the design and experimental implementation of controllers for hydraulic actuators is considered. Two different controllers are proposed. The first is an alternative backstepping controller, combined with feedback linearization. In this controller, the aim is to keep a simple control law minimizing the use of numerical differentiation (only one is necessary) and minimizing the error even in the presence of disturbances. The second is a linear two degree-of-freedom controller with pole placement minimizing a linear quadratic regulator performance index (the LQR-2DOF controller). This controller is robust to parameter variation and provides good disturbance rejection and noise attenuation properties. These controllers are tested in an experimental setup and the results are compared. Also, practical difficulties concerning the measurements of the variables to the both controllers are discussed.

In section 2, both a nonlinear and a linearised model of the hydraulic actuator are presented. The backstepping controller is designed in section 3 and the LQR-2DOF in section 4. In section 5, the experimental setup is described. Experimental results are shown and discussed in section 6. In section 7, the conclusions are presented.

2 Modelling of a Hydraulic Actuator

The hydraulic actuator shown in Fig. 1 consists of a single-rod cylinder controlled by a symmetrical critical-centre 4-way 2-stage servo valve.

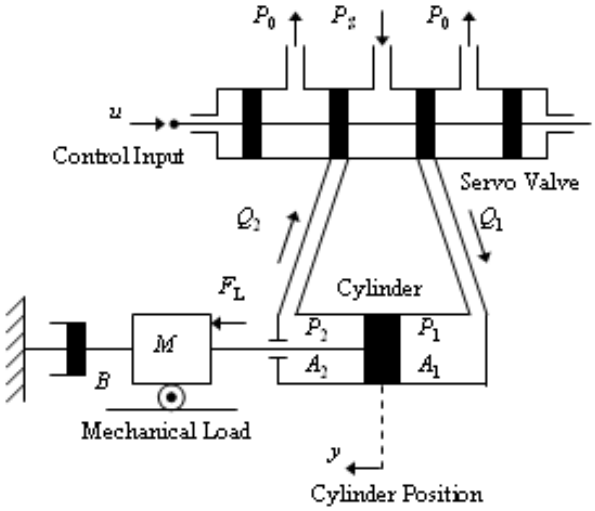

Fig. 1: *Servo Hydraulic Actuator*

In Fig. 1, P_S is the supply fluid pressure (supplied by a high-pressure fluid pump, not shown), P_0 is the reservoir pressure, P_1 and P_2 are the pressures in cylinder chambers 1 and 2, respectively, V_{h1} and V_{h2} are the initial volumes in chambers (and lines) 1 and 2, respectively, Q_1 is the fluid flow from the servo valve to chamber 1, Q_2 is the fluid flow from chamber 2 to the servo valve, M is the mass of the piston and the load coupled to the actuator, B is the viscous friction coefficient, A_1 is the cylinder piston cross-sectional area in chamber 1, A_2 is the cylinder piston cross-sectional area in chamber 2, u is the control input (the voltage applied to the servo valve), y is the piston position and F_L is an external force acting on the load. The origin of the system (the position $y = 0$) is chosen to be mid-cylinder.

2.1 Nonlinear Model

When a control input u is applied to the servo valve, it causes a displacement of the spool. This displacement, x_v, is considered directly proportional[1] to the control input u, i.e.,

$$x_v = K_{em} u \tag{1}$$

where K_{em} is the servo valve gain.

The displacement of the spool opens the passages of fluid to the chambers, causing the flows Q_1 and Q_2. These flows may be modelled by the "equation of flow through an orifice", yielding

$$Q_1 = \begin{cases} K x_v \sqrt{2(P_S - P_1)} & , \text{if } x_v \geq 0 \\ K x_v \sqrt{2(P_1 - P_0)} & , \text{if } x_v < 0 \end{cases} \tag{2}$$

$$Q_2 = \begin{cases} K x_v \sqrt{2(P_2 - P_0)} & , \text{if } x_v \geq 0 \\ K x_v \sqrt{2(P_S - P_2)} & , \text{if } x_v < 0 \end{cases} \tag{3}$$

where K is a hydraulic constant that depends on the flow discharge coefficient of the servo valve and on the diameter of the orifice[2].

According to the "Continuity Equation"', the pressures in chambers 1 and 2 have the following dynamics

$$\dot{P}_1 = \frac{\beta}{(V_{h1} + A_1 y)}(Q_1 - A_1 \dot{y}) \tag{4}$$

$$\dot{P}_2 = \frac{\beta}{(V_{h2} - A_2 y)}(A_2 \dot{y} - Q_2) \tag{5}$$

where β is the fluid bulk modulus.

The load dynamics is given by

$$M\ddot{y} + B\dot{y} = F_P + F_L \tag{6}$$

where $F_P = A_1 P_1 - A_2 P_2$ is the force applied by the piston on the load.

Combining the equations above, the nonlinear model of the hydraulic actuator is

[1] Valve dynamics are neglected. This assumption is acceptable because the bandwidth of the valve used in this work is much higher than the bandwidth of the actuator. As stated by Sohl and Bobrow (1999), only minimal performance improvement is achieved by including these dynamics in the control design.

[2] Eq. 2 and Eq. 3 are frequently used in literature. However, they are valid only for turbulent flow and not for the laminar flow that occurs when the valve is almost closed. If one desires to take into account this effect, a more complete model should be used (see Jelali and Kroll (2002)).

$$\begin{cases} M\ddot{y} + B\dot{y} = F_P + F_L \\ \dot{F}_P = \mathrm{d}(y, \dot{y}) + \mathrm{h}(y, P_1, P_2, x_v)u \end{cases} \quad (7)$$

with

$$\mathrm{d}(y, \dot{y}) = -\beta\left(\frac{A_1^2}{V_{h1} + A_1 y} + \frac{A_2^2}{V_{h2} - A_2 y}\right)\dot{y}$$

$$\mathrm{h}(y, P_1, P_2, x_v) = \frac{\beta K_{em}}{x_v}\left(\frac{A_1 Q_1}{V_{h1} + A_1 y} + \frac{A_2 Q_2}{V_{h2} - A_2 y}\right)$$

Further details on the modelling of hydraulic actuators may be found in Watton (1989) and in Merrit (1967).

2.2 Linearised Model

The system is linearised around the origin, thus $y \cong 0$.

Using the function signum of x_v and considering the reservoir pressure P_0 equal to 0, the flows Q_1 and Q_2 may be written as

$$\begin{aligned} Q_1 &= Kx_v\sqrt{P_S + \mathrm{sign}(x_v)(P_S - 2P_1)} \\ &\approx Kx_v\left(\sqrt{P_S} + \frac{\mathrm{sign}(x_v)(P_S - 2P_1)}{2\sqrt{P_S}}\right) \end{aligned} \quad (8)$$

$$\begin{aligned} Q_2 &= Kx_v\sqrt{P_S - \mathrm{sign}(x_v)(P_S - 2P_2)} \\ &\approx Kx_v\left(\sqrt{P_S} - \frac{\mathrm{sign}(x_v)(P_S - 2P_2)}{2\sqrt{P_S}}\right) \end{aligned} \quad (9)$$

The constants

$$K_Q = KK_{em}\sqrt{P_S} \quad (10)$$

$$K_C = \frac{Kx_v\,\mathrm{sign}(x_v)}{2\sqrt{P_S}} = \frac{K|x_v|}{2\sqrt{P_S}} \quad (11)$$

are defined. In practical applications, the value of K_C is obtained by identification, rather than calculated by the expression given above[3].

Making the changes given above in the nonlinear model, the linearised model of the hydraulic actuator is

$$\begin{cases} M\ddot{y} + B\dot{y} = A_1P_1 - A_2P_2 + F_L \\ \dot{P}_1 = \dfrac{\beta}{V_{h1}}\left(K_C(P_S - 2P_1) + K_Q u - A_1\dot{y}\right) \\ \dot{P}_2 = \dfrac{\beta}{V_{h2}}\left(K_C(P_S - 2P_2) - K_Q u + A_2\dot{y}\right) \end{cases} \quad (12)$$

2.3 Uncertainties and Disturbances

The parameters M, B, A_1, A_2, V_{h1} and V_{h2} may be determined with accuracy. However, the parameters β, P_S, K_C, K_Q, K and K_{em} may present variations during the operation of the system, such as:

- the high-pressure fluid pump does not supply a constant P_S,
- the presence of unsolved air in the lines and in the cylinder chambers decreases the value of β,
- variations in the temperature of the fluid cause variations in the value of β,
- K and K_{em} present small variations for different openings of the valve, and
- K_C and K_Q are valid next to the point of linearization.

F_L is considered as a disturbance acting on the system. This disturbance may be caused by extra load, by static friction and by Coulomb friction (the viscous friction is considered in the model).

3 Design of the Backstepping Controller

The backstepping controller is designed following the procedure described by Khalil (1996). Backstepping is a recursive Lyapunov-based procedure that breaks the design problem for the full system into a sequence of design problems for lower-order systems.

The state space representation of the nonlinear system described by Eq. 7, with state variables $x_1 = y$, $x_2 = \dot{y}$ and $x_3 = F_P$, is

$$\begin{cases} \dot{x}_1 = x_2 \\ \dot{x}_2 = -\dfrac{B}{M}x_2 + \dfrac{1}{M}x_3 + \dfrac{1}{M}F_L \\ \dot{x}_3 = \mathrm{d}(x_1, x_2) + \mathrm{h}(x_1, P_1, P_2, x_v)u \end{cases} \quad (13)$$

The control objective is trajectory tracking. The system output $y = x_1$ must track a reference trajectory y_d, with derivatives $\dot{y}_d$, $\ddot{y}_d$ and $\dddot{y}_d$.

Defining the errors $e_1 = x_1 - y_d$ and $e_2 = x_2 - \dot{y}_d$, the system is rearranged as

$$\begin{cases} \dot{e}_1 = e_2 \\ \dot{e}_2 = -\dfrac{B}{M}e_2 - \dfrac{B}{M}\dot{y}_d - \ddot{y}_d + \dfrac{1}{M}x_3 + \dfrac{1}{M}F_L \\ \dot{x}_3 = \mathrm{d}(e_1, e_2, y_d, \dot{y}_d) + \mathrm{h}(e_1, P_1, P_2, x_v, y_d)u \end{cases} \quad (14)$$

where e_1, e_2 and x_3 are the new state variables. For this new system, the objective is to stabilize the origin, that is, to vanish the error.

Initially, a feedback linearization control input is applied. This control input[4] is

$$u = \frac{1}{\mathrm{h}(e_1, P_1, P_2, x_v, y_d)}\left(u_a - \mathrm{d}(e_1, e_2, y_d, \dot{y}_d)\right) \quad (15)$$

where u_a is the backstepping control input to be determined.

Applying the control input u to system (Eq. 14) re-

[3] Eq. 11 results from a simplified model that neglects leakages in the valve and, for this reason, its analytical evaluation does not correspond to the value of K_C obtained by identification.

[4] Over the domain of interest, $\mathrm{h}(e_1, P_1, P_2, x_v, y_d) \neq 0$.

duces it to the integrator backstepping form, which is

$$\begin{cases} \dot{e}_1 = e_2 \\ \dot{e}_2 = -\dfrac{B}{M} e_2 - \dfrac{B}{M}\dot{y}_\mathrm{d} - \ddot{y}_\mathrm{d} + \dfrac{1}{M} x_3 + \dfrac{1}{M} F_\mathrm{L} \\ \dot{x}_3 = u_\mathrm{a} \end{cases} \tag{16}$$

Supposing that the subsystem

$$\begin{cases} \dot{e}_1 = e_2 \\ \dot{e}_2 = -\dfrac{B}{M} e_2 - \dfrac{B}{M}\dot{y}_\mathrm{d} - \ddot{y}_\mathrm{d} + \dfrac{1}{M} x_3 + \dfrac{1}{M} F_\mathrm{L} \end{cases} \tag{17}$$

may be stabilized by a smooth virtual control law

$$\tilde{x}_3 = M\left(\frac{B}{M}\dot{y}_\mathrm{d} + \ddot{y}_\mathrm{d} - \phi_1 e_1 + \left(\frac{B}{M} - \phi_2 \right) e_2 \right) \tag{18}$$

where ϕ_1 and ϕ_2 are state feedback gains, yields

$$\underbrace{\begin{bmatrix} \dot{e}_1 \\ \dot{e}_2 \end{bmatrix}}_{\dot{\boldsymbol{e}}} = \underbrace{\begin{bmatrix} 0 & 1 \\ -\phi_1 & -\phi_2 \end{bmatrix}}_{\mathbf{A_{MF}}} \underbrace{\begin{bmatrix} e_1 \\ e_2 \end{bmatrix}}_{\boldsymbol{e}} + \underbrace{\begin{bmatrix} 0 \\ 1/M \end{bmatrix}}_{\mathbf{D}} F_\mathrm{L} \tag{19}$$

The eigenvalues of matrix $\mathbf{A_{MF}}$ are closed-loop poles of the subsystem. The values of ϕ_1 and ϕ_2 are chosen accordingly in order to obtain the desired poles.

For the Lyapunov function $\mathrm{V}(\boldsymbol{e}) = \boldsymbol{e}^\mathrm{T}\mathbf{P}\boldsymbol{e}$, where $\mathbf{P}$ is a positive definite matrix[5], the time derivative is

$$\dot{\mathrm{V}}(\boldsymbol{e}, F_\mathrm{L}) = \boldsymbol{e}^\mathrm{T}\left[\mathbf{A}_\mathbf{MF}^\mathrm{T}\mathbf{P} + \mathbf{P}\mathbf{A}_\mathbf{MF}\right]\boldsymbol{e} + 2\boldsymbol{e}^\mathrm{T}\mathbf{P}\mathbf{D}F_\mathrm{L} \tag{20}$$

If F_L is bounded, i.e., $\|F_\mathrm{L}\| \le \theta$, for a positive constant θ, then making

$$\mathbf{A}_\mathbf{MF}^\mathrm{T}\mathbf{P} + \mathbf{P}\mathbf{A}_\mathbf{MF} = -\mathbf{Q} \tag{21}$$

for an adequate choice of the positive definite matrix $\mathbf{Q}$ leads to

$$\dot{\mathrm{V}}(\boldsymbol{e}, F_\mathrm{L}) \le \mathrm{W}(\boldsymbol{e}, F_\mathrm{L}) \tag{22}$$

where $\mathrm{W}(\boldsymbol{e},F_\mathrm{L})$ is positive definite. Thus, $\boldsymbol{e}$ is bounded[6]. The origin of the nominal subsystem, i.e., the subsystem with $F_\mathrm{L} = 0$, is asymptotically stable.

By adding and subtracting $(1/M)\tilde{x}_3$ on the right-hand side of the function $\dot{e}_2$ in system (Eq. 16) and defining the change of variables $z = x_3 - \tilde{x}_3$, which represents the error between the virtual control $\tilde{x}_3$ and the real control x_3, the equivalent representation of the system is obtained

$$\begin{cases} \dot{e}_1 = e_2 \\ \dot{e}_2 = -\phi_1 e_1 - \phi_2 e_2 + \dfrac{1}{M} F_\mathrm{L} + \dfrac{1}{M} z \\ \dot{z} = u_\mathrm{a} - \dot{\tilde{x}}_3 \end{cases} \tag{23}$$

The objective is to stabilize this system, minimizing the errors $\boldsymbol{e}$ and z. For the candidate Lyapunov function

$$\mathrm{V}_\mathrm{a}(\boldsymbol{e}, z) = V(\boldsymbol{e}) + \frac{1}{2} z^2 \tag{24}$$

the time derivative is

$$\dot{\mathrm{V}}_\mathrm{a} = \dot{\mathrm{V}} + z\left(\frac{2}{M}\left(\mathrm{p}_{12} e_1 + \mathrm{p}_{22} e_2\right) + u_\mathrm{a} - \dot{\tilde{x}}_3 \right) \tag{25}$$

Choosing the backstepping control input

$$u_\mathrm{a} = \dot{\tilde{x}}_3 - \frac{2}{M}\left(\mathrm{p}_{12} e_1 + \mathrm{p}_{22} e_2\right) - \mathrm{c}z \tag{26}$$

where c is a positive constant, and considering the result (Eq. 22), yields

$$\dot{\mathrm{V}}_a \le -\mathrm{W}(\boldsymbol{e}, F_\mathrm{L}) - \mathrm{c}z^2 < 0 \tag{27}$$

which shows that the system (Eq. 23) is stable and that $\boldsymbol{e}$ and z are uniformly ultimately bounded (Qu and Dawson, 1995). The evaluation of the set to which the tracking error converges and its relationship with the parameter variations is an open problem.

Substituting Eq. 18 in Eq. 26, yields

$$\begin{aligned} u_\mathrm{a} = {} & \mathrm{c}M\left(\frac{B}{M}\dot{y}_\mathrm{d} + \ddot{y}_\mathrm{d} - \phi_1 e_1 + \left(\frac{B}{M} - \phi_2 \right) e_2 \right) + \\ & + M\left(\frac{B}{M}\ddot{y}_\mathrm{d} + \dddot{y}_\mathrm{d} - \phi_1 e_2 + \left(\frac{B}{M} - \phi_2 \right)\dot{e}_2 \right) + \\ & - \frac{2}{M}\left(\mathrm{p}_{12} e_1 + \mathrm{p}_{22} e_2\right) + \mathrm{c}x_3 \end{aligned} \tag{28}$$

The combination of Eq. 15 and Eq. 28 gives the complete control law for the system.

For the experimental setup described in section 5, whose nominal values of the parameters are given in Table 1, two fast poles are chosen, in order to guarantee a fast convergence. These poles are p_1 = -50 and p_2 = -400. Therefore, the gains ϕ_1 and ϕ_2 are ϕ_1 = 20000 and ϕ_2 = 450. Substituting the known values in Eq. 28, yields

$$\begin{aligned} u_\mathrm{a} = {} & 316\mathrm{c}\dot{y}_\mathrm{d} + (316 + 20.66\mathrm{c})\ddot{y}_\mathrm{d} + 20.66\dddot{y}_\mathrm{d} + \\ & + (413200\mathrm{c} - 0.0968\mathrm{p}_{12})e_1 - 8981\dot{e}_2 + \\ & - (413200 + 0.0968\mathrm{p}_{22} + 8981\mathrm{c})e_2 \end{aligned} \tag{29}$$

According to this expression, the contribution of p_{12} and p_{22} to the control signal is very small. In fact, it is almost imperceptible. Matrix $\mathbf{Q}$ is randomly chosen to be [1000 0;0 1000], then p_{12} = 0.025 and p_{22} = 1.1112. The positive constant c is chosen to be 500.

The signals that have to be measured to implement the backstepping controller are the piston position, velocity and acceleration, the servo valve spool position and the pressure difference. For practical purposes the measurement of acceleration is not desired. In particular, the acceleration obtained from numerical differentiation can lead to bad results due to the presence of noise. An efficient way to circumvent this problem is to design a controller with similar performance employing a reduced number of measured signals. It is possible to achieve this goal with a linear control approach. Unlike

[5] Matrix $\mathbf{P}$ has the form $\begin{bmatrix} \mathrm{p}_{11} & \mathrm{p}_{12} \\ \mathrm{p}_{12} & \mathrm{p}_{22} \end{bmatrix}$.

[6] Proof of this result may be found in Khalil (1996), chapter 5.

classical controllers, the LQR-2DOF controller allows an optimized pole placement for this system, ensuring high performance and being, at the same time, robust to parameter variations and external disturbances.

4 Design of the LQR-2DOF Controller

The LQR-2DOF controller[7] is designed following the procedure described by Wolovich (1995). This controller allows the closed-loop system to maintain a desired response performance while varying the loop performance, which means that it is possible to improve robust stability, disturbance rejection and noise attenuation, independently of response performance.

Applying the Laplace Transform in Eq. 12 and substituting the values from Table 1, the linearised system transfer function[8] is

$$y(s) = \underbrace{\frac{c(s)}{a(s)}}_{G(s)} u(s) + d(s) \tag{30}$$

with

$$c(s) = 17720$$

$$a(s) = s^3 + 75s^2 + 117190s$$

$$d(s) = \frac{0.05(s+60)}{s^3 + 75s^2 + 117190s} F_L(s)$$

where $G(s)$ is a transfer function from input to output and $d(s)$ is a disturbance signal added to the output. The open-loop poles are 0 and -37.5 ± 340.3j.

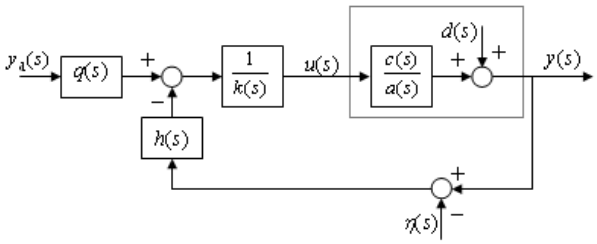

Fig. 2: *Closed-Loop System*

The LQR-2DOF controller has the configuration shown in Fig. 2, where the polynomials[9]

$$\begin{aligned} q(s) &= q_2 s^2 + q_1 s + q_0 \\ h(s) &= h_2 s^2 + h_1 s + h_0 \\ k(s) &= s^2 + k_1 s + k_0 \end{aligned} \tag{31}$$

are to be determined to achieve the desired closed-loop goals.

The closed-loop system is given by

$$y(s) = T(s) y_d(s) + S(s) d(s) + C(s) \eta(s) \tag{32}$$

with

$$T(s) = \frac{c(s)q(s)}{\delta(s)}$$

$$S(s) = \frac{a(s)k(s)}{\delta(s)}$$

$$C(s) = \frac{c(s)h(s)}{\delta(s)}$$

$$\delta(s) = a(s)k(s) + c(s)h(s)$$

where $T(s)$ is the output response transfer function, $S(s)$ is the sensitivity transfer function and $C(s)$ is the complementary sensitivity transfer function. $\delta(s)$ is the characteristic polynomial, whose 5 roots are the closed-loop poles. The overall performance of the system depends on the ability of its output $y(t)$ to track the reference input $y_d(t)$ while minimizing the effect of both the disturbance signal $d(t)$ and the sensor noise $\eta(t)$ on its behaviour.

$T(s)$ should guarantee that the output response presents some desired characteristics, such as a small settling time and no overshoot.

A choice of arbitrary stable polynomials $q_m(s)$ and $\delta_m(s)$, such that

$$q(s) = \alpha q_m(s) \tag{33}$$

$$\delta(s) = \delta_m(s) q_m(s) \tag{34}$$

causes zero-pole cancellations, yielding

$$T(s) = \frac{c(s)q(s)}{\delta(s)} = \frac{\alpha c(s)}{\delta_m(s)} \tag{35}$$

Therefore $\delta_m(s)$ contains the 3 poles that define the nominal output response and $q_m(s)$ contains the 2 poles that only affect $S(s)$ and $C(s)$.

The 3 poles of $\delta_m(s)$ are chosen using the LQR performance index, defined by

$$J_{LQR} = \int_0^\infty \left(\rho y^2(t) + u^2(t)\right) \tag{36}$$

where ρ is an weighting factor. The minimization of J_{LQR} implies the minimization of both excessive output $y(t)$ excursions and control efforts $u(t)$ required to prevent such excursions. The poles of $\delta_m(s)$ that minimize the index are found using the Spectral Factorization Method. These poles are the 3 negative roots of

$$\Delta(s) = a(s)a(-s) + \rho c(s)c(-s) \tag{37}$$

for some real $\rho > 0$.

In order to choose the closed-loop poles, the root-

[7] A linear two degree-of-freedom controller with pole placement minimizing a linear quadratic regulator performance index.

[8] In the particular experimental setup used, $A_1 = A_2$ and $V_{h1} = V_{h2}$. For this reason, there is not a term depending on P_S in the linearised system transfer function. In the more general case, one can use a control law $u(s) = u_{2DOF}(s) + u_{Ps}(s)$, where $u_{Ps}(s)$ compensates the term depending on P_S and $u_{2DOF}(s)$ is calculated according to the procedure described in this section.

[9] These polynomials have degrees equal to (deg[$a(s)$]-1) and $k(s)$ is monic.

square locus[10] of $\Delta(s)$, shown in Fig. 3, is used. According to the Fig. 3, the two negative complex conjugate poles are far from the real axis and not so close to the imaginary axis. Therefore, they have only a small influence on the output and the system dynamics is dominated by the negative real pole. The system behaves approximately as a first order system, with some oscillations. The negative real pole is chosen to ensure that the 2% settling time t_s is 0.02 s. Thus, this pole[11] is equal to -200. Consequently, $\rho = 3.14\times10^6$, the other two poles are -105 ± 382j and

$$\delta_m(s) = s^3 + 410s^2 + 198949s + 31389800 \tag{38}$$

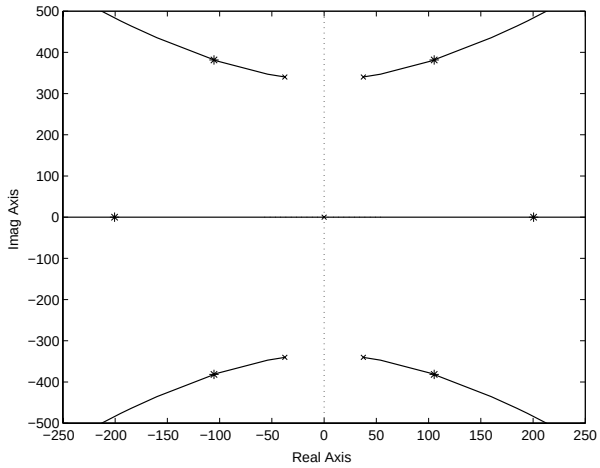

Fig. 3: *Root-Square Locus of Δ(s)*

In order to guarantee a DC gain of the output response transfer function (Eq. 35) equal to 1,

$$\alpha = \frac{\delta_m(0)}{c(0)} = \frac{31389800}{17720} = 1772 \tag{39}$$

$S(s)$ should provide disturbance rejection and $C(s)$ should provide noise attenuation. In order to accomplish that, $|S(j\omega)|$ should be minimized over the band of frequencies that characterizes $d(t)$ and $|C(j\omega)|$ should be minimized over the frequencies that characterizes $\eta(t)$.

An additional desired characteristic for $S(s)$ is that

$$\|S\|_\infty = \max_\omega |S(j\omega)| \le 2 \approx 6\text{dB} \tag{40}$$

ensuring robust stability with respect to plant parameter variations, as demonstrated by Wolovich (1995).

In Fig. 4, Bode plots of two different disturbance signals $d(s)$ are shown. In the first one the external force F_L is a step of amplitude 1000N and in the second one F_L is a sine wave of amplitude 1000N and frequency 1 Hz. It can be seen that the disturbance signal is characterized by low frequencies. The noise $\eta(t)$ in this system is characterized by high frequencies. Thus, the desired behaviour for $S(s)$ and $C(s)$, considering that they are complementary and not independent, is

$$|S(j\omega)| \approx \begin{cases} 0 \text{ at low } \omega \\ 1 \text{ at high } \omega \end{cases} \tag{41}$$

$$|C(j\omega)| \approx \begin{cases} 1 \text{ at low } \omega \\ 0 \text{ at high } \omega \end{cases}$$

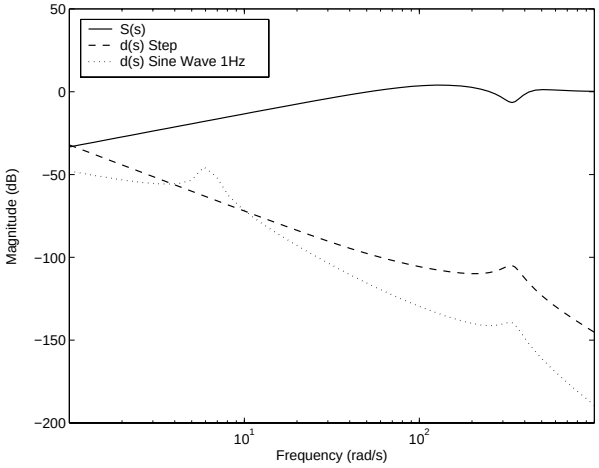

Fig. 4: *Bode Diagram of S(s) and d(s)*

The polynomial $q_m(s)$ is chosen to be $s^2+400s+39900$ (the poles are -190 and -210). This choice guarantees an acceptable behaviour for $S(s)$ and $C(s)$, as seen in Fig. 4 and Fig. 5. Using the value of α obtained in Eq. 39,

$$q(s) = 1772s^2 + 708919s + 70714646 \tag{42}$$

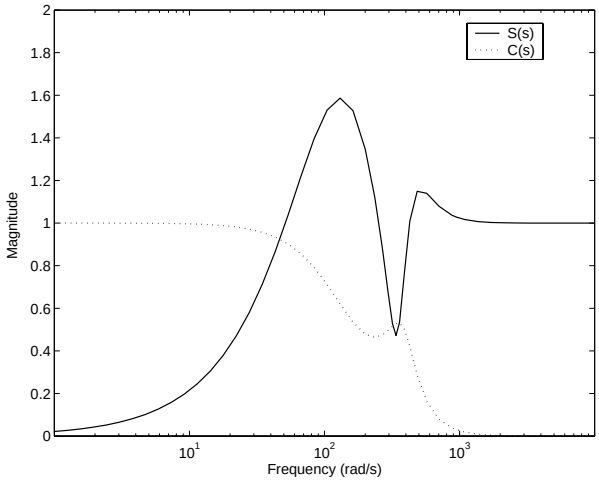

Fig. 5: *Magnitude Diagram of S(s) and C(s)*

The polynomials $h(s)$ and $k(s)$ are obtained solving the so-called *Diophantine equation*

$$\delta(s) = a(s)k(s) + c(s)h(s) \tag{43}$$

Thus

$$h(s) = 1342s^2 - 369486s + 70714646 \tag{44}$$

$$k(s) = s^2 + 736s + 230781 \tag{45}$$

The LQR-2DOF controller is composed by polynomials (Eq. 42, 44 and 45). The only signal that has to be measured to implement this controller is the piston position.

[10] The root-square locus is an s-plane plot of all roots of Δ(s), as ρ varies from 0 to ∞.

[11] For a first order system, $t_s = 4\tau$, where τ is the system time constant, and the only pole is given by $-1/\tau$.

5 Experimental Setup

In this section, the particular system where the experimental implementation of the controllers was carried out is described. This hydraulic system is installed on LASHIP (in the Federal University of Santa Catarina, Brazil).

The experimental setup consists of:

- a symmetric double-acting-double-ended cylinder,
- a servo valve and its electronic card,
- position transducers,
- temperature transducers in each cylinder chamber,
- pressure transducers in each cylinder chamber,
- a *DS*1102 board, responsible for the data acquisition and the control signal generation, and
- a computerized hydraulic power and conditioning unit, which maintains the fluid at the required conditions.

The nominal parameters of the system are given in Table 1. These parameters were obtained from manufacturers and experimental data. Since the cylinder is double ended and symmetric, $A_1 = A_2$ and $V_{h1} = V_{h2}$.

Table 1: Nominal Parameters

Parameter	Nominal Value
M	20.66 kg
B	316 Ns/m
A_1	7.6576×10^{-4} m^2
A_2	7.6576×10^{-4} m^2
V_{h1}	4.882×10^{-4} m^3
V_{h2}	4.882×10^{-4} m^3
β	10^9 N/m^2
P_S	10^7 N/m^2
K_C	1.46×10^{-11} m^6/VsN
K_Q	1.167×10^{-4}m^3/Vs
KK_{em}	3.97×10^{-8} m^4/VsN$^{0.5}$

The saturation limits for u are -10V and 10V and for y are -0.5 m and 0.5 m.

6 Experimental Results

The backstepping controller and the LQR-2DOF controller were tested in the experimental setup described in section 5, using the *Euler* integration method with a fixed step of 1ms. The control algorithms were developed using *Matlab/Simulink* and then loaded into the DS1102 board. All measured signals were filtered by low pass filters with cut-off frequencies of 100rad/s, due to the presence of noise. The signals obtained by numerical differentiation (piston velocity and acceleration) were also filtered, since the differentiation process amplifies the noise.

During the operation of the system, P_S presented variations of ±30% of its nominal value. The fluid temperature was kept between 40 and 45 degrees Celsius, consequently, small changes in β were expected.

The experimental results are presented in Fig. 6, Fig. 7, Fig. 8 and Fig. 9. In each figure, the first plot shows the output response, the second plot shows the tracking error and the third plot shows the control input.

6.1 Sine Wave Tracking

In Fig. 6, the reference y_d is a sine wave with frequency 0.5 Hz, varying from -0.4m to 0.4m. The maximum error for the backstepping controller is 3.5mm, while the maximum error for the LQR-2DOF controller is 11mm.

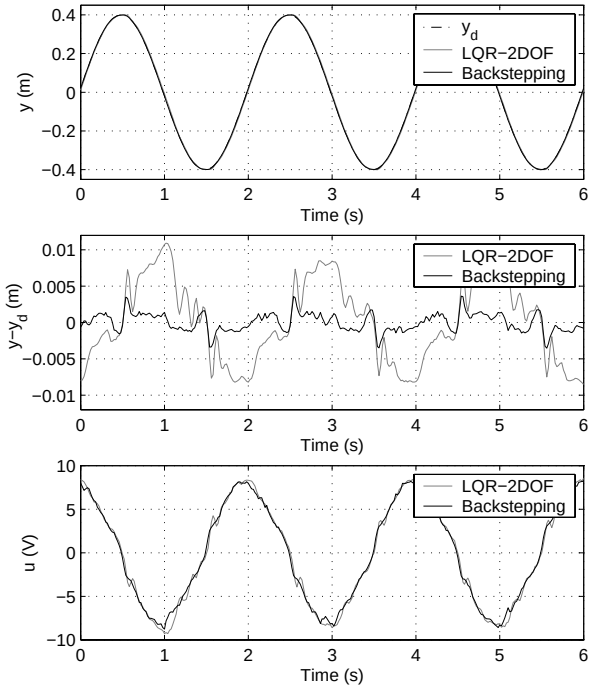

Fig. 6: *Sine Wave Tracking (0.5Hz)*

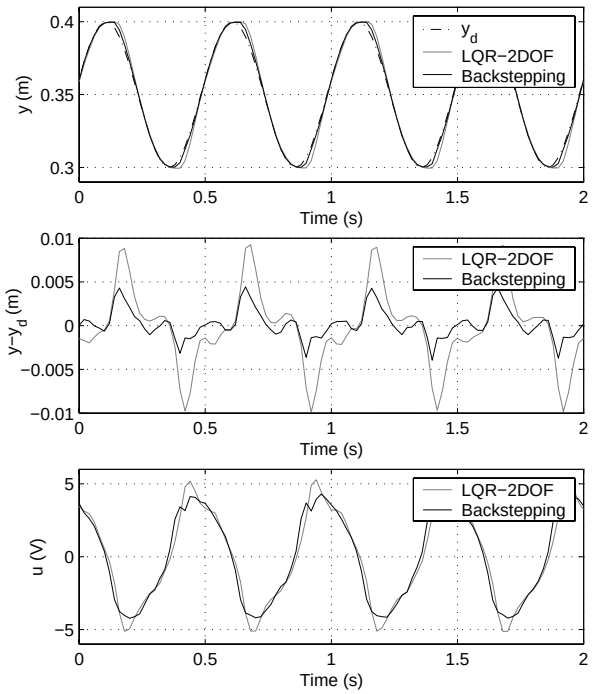

Fig. 7: *Sine Wave Tracking (2Hz)*

In Fig. 7, the reference y_d is a sine wave with frequency 2 Hz, varying from 0.3 m to 0.4 m. The maximum error for the backstepping controller is 4.5 mm, while the maximum error for the LQR-2DOF controller is 10 mm. In both cases, there is no phase lag and the control signal is smooth.

6.2 Step Response

In Fig. 8, the reference y_d is a sequence of steps, each one with amplitude 0.2 m. In this case, there is a saturation of the control signal, i.e., the actuator moves with maximum velocity. Not considering the saturated portion, the LQR-2DOF controller presents overshoot of 20 mm, while the backstepping controller does not have overshoot.

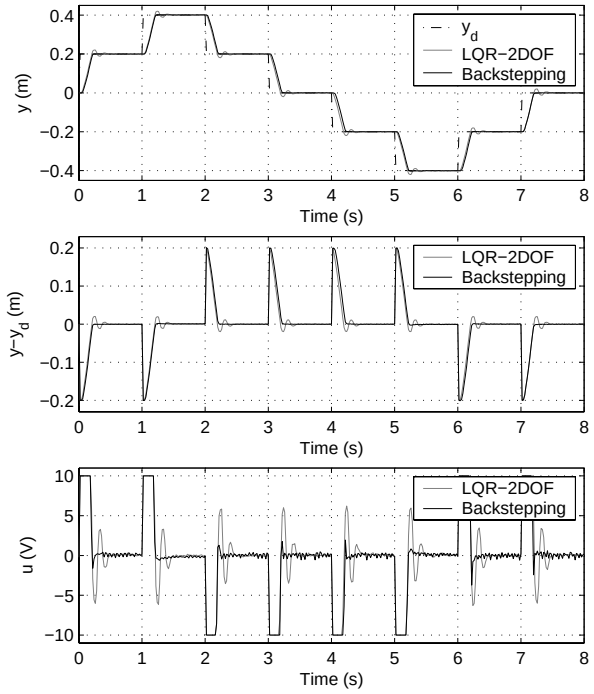

Fig. 8: *Step Response*

6.3 Polynomial Trajectory Tracking

In Fig. 9, the reference y_d is a smooth polynomial trajectory, varying from -0.4 m to 0.4 m. The maximum error for the backstepping controller is 4 mm, while the maximum error for the LQR-2DOF controller is 6mm.

Considering these results, it follows that both controllers provide good trajectory tracking for low frequency sinusoidal inputs, step inputs and polynomial inputs, although the output response obtained with the LQR-2DOF presented in all cases a slightly bigger tracking error than the output response obtained with the backstepping controller. Nevertheless, these errors (when compared to the trajectories) are not very significant for many applications. Furthermore, both controllers show robustness to parameter variations, since the experiments were performed in non-nominal conditions (variations in P_S and β). In the actual stage of this work, the robustness to load variations was not verified due to limitations in the experimental set-up.

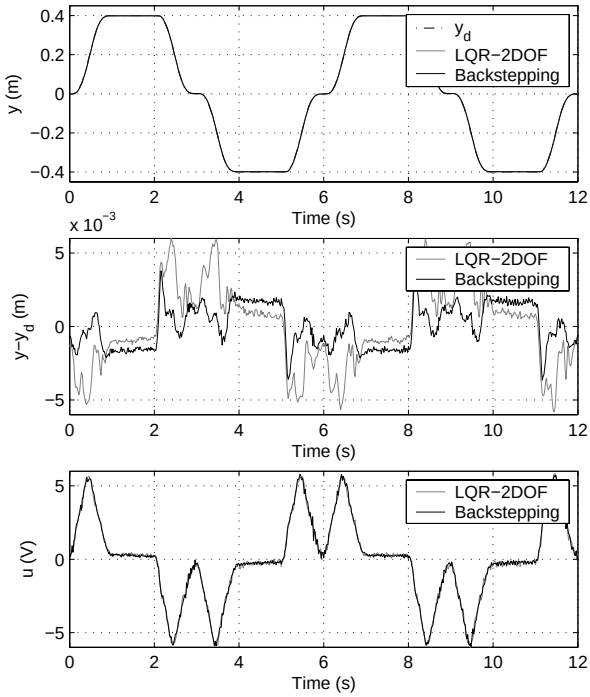

Fig. 9: *Polynomial Trajectory Tracking*

7 Conclusions

In this paper, the control of hydraulic actuators was presented. Two main aspects were considered: the robustness problem and the practical implementation problem. The experimental results show that the backstepping technique is a good way to improve high performance and to reduce tracking errors for the considered system. However, the complexity of the controller leads to a practical restriction: the acceleration measurement. The LQR-2DOF controller offers an efficient way to guarantee robustness and performance and is simpler to implement. The experimental results show that its performance is comparable to the backstepping controller performance, with a slightly bigger error.

The problem of friction compensation can lead to steady state errors and, as pointed out by some authors, limit cycles may occur. In the experimental results the relation between friction and these phenomena was not observed. Depending on the required performances this problem needs to be addressed.

Acknowledgements

The authors would like to thank the anonymous reviewers for their helpful comments and for the recommended references on uniformly ultimately bounded stability and on the mathematical model of the flow.

Nomenclature

A_1	cross-sectional area in chamber 1	[m²]
A_2	cross-sectional area in chamber 2	[m²]
B	viscous friction coefficient	[Ns/m]
F_L	external force acting on the load	[N]
F_P	force applied by piston on load	[N]
K	flow discharge coefficient	[$m^3/sN^{½}$]
K_{em}	servo valve gain	[m/V]
K_C	flow-pressure gain	[m^6/VsN]
K_Q	flow gain	[m^3/Vs]
M	mass of piston and load	[kg]
P_0	reservoir pressure	[N/m²]
P_1	pressure in cylinder chamber 1	[N/m²]
P_2	pressure in cylinder chamber 2	[N/m²]
P_S	supply fluid pressure	[N/m²]
Q_1	fluid flow: servo valve - chamber 1	[m^3/s]
Q_2	fluid flow: chamber 2 - servo valve	[m^3/s]
u	voltage applied to the servo valve	[V]
V_{h1}	initial volume in chamber 1	[m^3]
V_{h2}	initial volume in chamber 2	[m^3]
x_v	displacement of servo valve spool	[m]
y	actuator piston position	[m]
y_d	Reference trajectory	[m]
β	fluid bulk modulus	[N/m²]

References

Bobrow, J. E. and **Lum, K.** 1995. Adaptive, high bandwidth control of a hydraulic actuator. *Proceedings of the American Control Conference*, pp. 71-75.

Edge, K. A. 1997. The control of fluid power systems - responding to the challenges. *Proceedings Inst. Mechanical Engineers*, Vol. 211, pp. 91-110.

Fialho, I. and **Balas, G.** 1998. Adaptive vehicle suspension design using LPV methods. *Proceedings of the 37th IEEE Conference on Decision and Control*, pp. 2265-2270.

Guenther, R., **Cunha, M. A. B.** and **De Pieri, E. R.** 1998. Experimental implementation of the variable structure adaptive cascade control for hydraulic actuators. *Power Transmission and Motion Control*, pp. 349-361.

Guenther, R., **Cunha, M. A. B.**, **De Pieri, E. R.** and **De Negri, V. J.** 2000. VS-ACC applied to a hydraulic actuator. *Proceedings of American Control Conference*, pp. 4124-4128.

Heintze, H. 1997. *Design and Control of a Hydraulically Actuated Industrial Brick Laying Robot.* PhD thesis, Delft University of Technology.

Jelali, M. and **Kroll, A.** 2002. *Hydraulic Servo-Systems*. Springer.

Jovanović, M. 2002. Nonlinear control of an electro hydraulic velocity servo system. *Proceedings of American Control Conference*, pp. 588-593.

Khalil, H. K. 1996. *Nonlinear Systems*. Prentice Hall.

Merrit, H. E. 1967. *Hydraulic Control Systems*. Wiley and Sons.

Qu, Z. and **Dawson, D.** 1995. *Robust Tracking Control of Robot Manipulators.* IEEE Press.

Rudas, I. J., **Tar, J. K.**, **Bitó, J. F.** and **Kozlowski, K.** 2003. Improvement of a nonlinear adaptive controller designed for strongly nonlinear plants. *Proceedings of the 11th International Conference on Advanced Robotics*, pp. 1381-1386.

Sirouspour, M. R. and **Salcudean, S. E.** 2000. On the nonlinear control of hydraulic servo systems. *Proceedings of the IEEE International Conference on Robotics and Automation*, San Francisco.

Sohl, G. A. and **Bobrow, J. E.** 1999. Experiments and simulations on the nonlinear control of a hydraulic servo system. *IEEE Transactions on Control Systems Technology*, Vol. 7, No. 2, pp. 238-247.

Wang, J. and **Wilson, D. A.** 2001. Multi-objective control of decoupled vehicle suspensions systems. *Proceedings of the 41th IEEE Conference on Decision and Control*, pp. 535-540.

Watton, J. 1989. *Fluid Power Systems: Modelling, Simulation, Analog and Microcomputer Control*. Prentice Hall.

Wolovich, W. A. 1995. *Automatic Control Systems: Basic Analysis and Design*. Saunders College Publishing.

Yao, B., **Bu, F.** and **Chiu, G. T. C.** 1998. Nonlinear adaptive robust control of electro-hydraulic actuator servo systems with discontinuous projections. *Proceedings of the 37th IEEE Conference on Decision and Control*, pp. 2265-2270.

Yao, B., **Bu, F.**, **Reedy, J.** and **Chiu, G. T. C.** 2000. Adaptive robust motion control of single-rod hydraulic actuators: theory and experiments. *IEEE/-ASME Transactions on Mechatronics*, Vol. 5, No. 1, pp. 79–91.

Ana Lúcia Driemeyer Franco
Was born in Porto Alegre, Brazil, in 1977. She received the Automation and Control Engineering degree, in 2000, and the M.Sc. degree in Electrical Engineering, in 2002, both from UFSC, Brazil. At the moment, she is pursuing Doctoral degrees from EDSP/ENS/Cachan, France, and UFSC, Brazil, in a co-tutorship agreement.

Edson Roberto De Pieri
Was born in Mogi Mirim, Brazil, in 1960. He received the Mathematics degree, in 1982, and the M.Sc. degree in Electrical Engineering, in 1987, both from UNICAMP, Brazil. In 1991, he received the D.Sc. degree from the Pierre et Marie Curie University, France. Since 1992, he is professor at the Department of Automation and Systems at UFSC.

Eugênio Bona Castelan
Was born in Criciúma, Brazil. He received the Electrical Engineering degree, in 1982, and the M.Sc. degree, in 1985, both from UFSC, Brazil, and the Doctoral degree from Paul Sabatier University, France, in 1992. In 1993, he joined the Department of Automation and Systems at UFSC, where he develops his teaching and research activities.

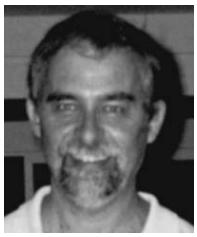

Raul Guenther
Was born in Joinville, Brazil, in 1953. He received the Mechanical Engineering degree, in 1976, from UFSC, Brazil, and the D.Sc. in Mechanical Engineering, in 1993, from UFRJ, Brazil. Since 1977, he is professor at the Department of Mechanical Engineering at UFSC. At the moment, he is the head of the Robotics Laboratory.

Antonio Carlos Valdiero
Was born in Volta Redonda, Brazil, in 1969. He received the Mechanical Engineering degree, in 1992, from UFRJ, Brazil, and the M.Sc. Degree, in 1994, from UFSC, Brazil. At the moment, he is pursuing a Doctoral degree in Mechanical Engineering from UFSC. Since 1994, he is professor at the Technology Department at UNIJUÍ, Brazil.